Received: 20 February 2019 | Revised: 29 May 2019 | Accepted: 28 June 2019

DOI: 10.1111/psyp.13442

ORIGINAL ARTICLE

PSYCHOPHYSIOLOGY SPR WILEY

Alpha-band desynchronization reflects memory-specific processes during visual change detection

Molly A. Erickson[1] | **Dillon Smith**[1] | **Matthew A. Albrecht**[2] | **Steven Silverstein**[1]

[1]Department of Psychiatry and University Behavioral Health Care, Rutgers University, Piscataway, New Jersey

[2]School of Public Health, Curtin University, Perth, Australia

Correspondence
Molly A. Erickson, Department of Psychiatry and University Behavioral Health Care, Rutgers University, 671 Hoes Lane West, Piscataway, NJ 08854.
Email: molly.erickson@rutgers.edu

Abstract

Recent work investigating physiological mechanisms of working memory (WM) has revealed that modulation of alpha and beta frequency bands within the EEG plays a key role in WM storage. However, the nature of that role is unclear. In the present study, we examined event-related desynchronization of alpha and beta (α/β-ERD) elicited by visual tasks with and without a memory component to measure the impact of a WM demand on this electrophysiological marker. We recorded EEG from 60 healthy participants while they completed three variants on a typical change detection task: one in which participants passively viewed the sample array, passive (WM−); one in which participants viewed and attended the sample array in search of a target color but did not memorize the colors, active (WM−); and one in which participants encoded, attended to, and memorized the sample array, active (WM+). Replicating previous findings, we found that active (WM+) elicited robust α/β-ERD in frontal and posterior electrode clusters and that α-ERD was significantly associated with WM capacity. By contrast, α/β-ERD was significantly smaller in the passive (WM−) and active (WM−) tasks, which did not consistently differ from one another. Furthermore, no such relationship was observed between WM capacity and desynchronization in the passive (WM−) or active (WM−) tasks. Taken together, these results suggest that α-ERD during memory formation reflects a memory-specific process such as consolidation or maintenance, rather than serving a generalized role in perceptual gating or engagement of attention.

KEYWORDS

alpha oscillations, beta oscillations, EEG, individual differences, visual working memory

1 | INTRODUCTION

Visual working memory (WM) capacity refers to the maximum number of visual items that one can maintain in memory at a given time. Interest in individual differences in WM capacity is motivated by evidence that it is significantly associated with overall cognitive ability (Cowan et al., 2005; Engle, Tuholski, Laughlin, & Conway, 1999). Indeed, WM capacity has been considered a core cognitive function, forming the basis of fluid, goal-directed behavior (e.g., Fukuda, Vogel, Mayr, & Awh, 2010). Due in part to its fundamental role across cognitive domains, it is of particular interest to identify the neurophysiological mechanisms that give rise to successful WM storage. Recently, there has been growing interest in the role of alpha (9–13 Hz) and beta (14–30 Hz) modulation within the EEG during WM tasks. A number of studies have reported robust event-related desynchronization of alpha and beta (α/β-ERD) following the onset of a visual array of stimuli to be memorized, which is associated with successful recall for those items among healthy individuals

at test (Astrand, 2018; Bashivan, Bidelman, & Yeasin, 2014; Chen, Chen, Kuang, & Huang, 2015; Foster, Sutterer, Serences, Vogel, & Awh, 2016; Fukuda, Mance, & Vogel, 2015; Pavlov & Kotchoubey, 2017; Sauseng et al., 2009; van Dijk, van der Werf, Mazaheri, Medendorp, & Jensen, 2010; Zammit, Falzon, Camilleri, & Muscat, 2018). Furthermore, disrupted α/β-ERD has been observed in clinical samples with known WM capacity impairments such as schizophrenia and attention deficit hyperactivity disorder (Erickson, Albrecht, Robinson, Luck, & Gold, 2017; Lenartowicz, Mazaheri, Jensen, & Loo, 2018). Taken together, α/β-ERD during memory formation and maintenance appears to be directly linked to the quantity or quality of those representations, and failure of this mechanism constrains WM capacity in certain forms of psychopathology.

Although an association between α/β-ERD and visual WM capacity has been clearly established, the precise function that it serves to facilitate memory storage is not yet known. There are several overlapping subprocesses necessary for successful WM function, including perception/encoding, attentional control, consolidation/storage, maintenance, and retrieval—any of which may be supported by this α/β-ERD mechanism. Importantly, a typical change detection paradigm cannot distinguish between these subprocesses required for successful task performance. The goal of the present study was therefore to determine whether α/β-ERD serves a memory-specific function (e.g., consolidation and maintenance) or if it is linked to other subprocesses that are necessary, but not sufficient, for successful WM task performance (e.g., perception and sustained attention). To do this, we systematically varied task demands while participants viewed a prototypical change detection paradigm sequence (Luck & Vogel, 1997). If α/β-ERD plays a unique role in memory formation, then it should be most robustly observed under task conditions in which participants are asked to remember the colors of the sample array. By contrast, others have conceptualized α/β-ERD as serving a more generalized "gating" function, passing task-relevant information through the visual stream for further processing when it is desynchronized and suppressing task-irrelevant information when it is highly synchronized (Handel, Haarmeier, & Jensen, 2011; Jensen & Mazaheri, 2010; Poch, Valdivia, Capilla, Hinojosa, & Campo, 2018; Zumer, Scheeringa, Schoffelen, Norris, & Jensen, 2014). Such a gating mechanism would be considered a function that is necessary, but not sufficient, for WM storage, and, indeed, some studies have demonstrated that α/β-ERD is elicited in response to visual stimuli during a task with no explicit memory component at all (e.g., Banerjee, Snyder, Molholm, & Foxe, 2011; Foster et al., 2016; Gomar et al., 2015; Handel et al., 2011; Ichihara-Takeda et al., 2015; Roijendijk, Farquhar, van Gerven, Jensen, & Gielen, 2013). These observations suggest the possibility that α/β-ERD reflects engagement of earlier more generalized visual processes, such as perceptual encoding or modulation of attention. In this case, robust α/β-ERD should be observed even in the absence of task instructions to memorize the visual stimuli.

To test this hypothesis, we developed a task using three variants on a visual change detection paradigm while EEG was recorded. In the passive (WM−) task variant, participants passively viewed sample arrays of 2, 4, or 6 colored squares, without any instruction to attend to or remember the colors. In the active (WM−) task variant, participants actively viewed sample arrays of 2, 4, or 6 colored squares by searching the arrays for a predetermined target color, which remained continuously present at the top of the screen but without any instruction to remember the colors. Finally, in the active (WM+) task variant, participants actively viewed the sample arrays of 2, 4, or 6 colored squares and consolidated them for memory storage during a delay period of 2,000 ms. These tasks were therefore perceptually identical to one another, with the exception of the continuously present reference square during the active (WM−) paradigm; the only difference between tasks was the nature of the cognitive demand. α/β-ERD was measured from frontal and posterior electrode clusters, and the correlation between WM capacity and α/β-ERD magnitude was examined separately for each task variant.

2 | METHOD

2.1 | Participants and assessment measures

Sixty-six individuals were recruited from Rutgers University and the surrounding community to participate in the present study. Six participants were removed from analysis following artifact rejection procedures (see below) in which fewer than 50% of data epochs were retained. The demographic information for the remaining 60 participants is presented in Table 1. All participants were between the ages of 18–60, self-reported that they were free from a history of serious mental illness and neurologic injury, and had normal or corrected-to-normal vision. To obtain a brief measure of cognitive ability,

TABLE 1 Demographic information

	Sample characteristics
Age, years	35.85 (13.58)
Gender (male:female)	24:36
Race (AA:A:C:O)	11:23:24:2
Education, years	15.82 (1.93)
Parental education, years	14.26 (2.97)
WASI IQ[a]	106.60 (11.94)

Note: ($N = 60$).
Abbreviations: AA, African American; A, Asian; C, Caucasian; O, other; WASI, Wechsler Abbreviated Scale of Intelligence.
[a]WASI IQ missing for two participants.

the two-subtest version of the Wechsler Abbreviated Scale of Intelligence (Wechsler, 2011) was also administered. All recruiting methods and experimental procedures were approved by the Rutgers University Institutional Review Board.

2.2 | Experimental paradigm

Stimuli were presented on a liquid crystal display monitor with a gray background (x = .324, y = .348, 164.0 cd/m^2) and a continuously visible central fixation cross at a nominal viewing distance of 100 cm. For all three task variants, passive (WM−), active (WM−), and active (WM+), each trial began with a blank prestimulus period of 1,500 ms, followed by an array of 2, 4, or 6 colored squares that appeared for 200 ms. In the active (WM−) condition, this blank prestimulus interval included the continuously present reference square positioned at the top of the screen. The squares were arranged around an invisible circle with a radius of 4.1 degrees, and each square measured 0.66 × 0.66 degrees visual angle. The colors of the squares in the array were highly discriminable and selected randomly and without replacement from a list of the following colors (RGB values in parentheses): dark brown (140,81,10), tan (216,179,101), magenta (197,27,125), light pink (233,163,201), yellow (255,255,0), sage (161,215,106), teal (77,146,33), midnight blue (1,102,94), and sky blue (90,180,172). This array was followed by a blank delay period of 2,000 ms (see Figure 1 for the sequence of each trial type).

In the active (WM+) task variant (Figure 1c), this 2,000-ms delay interval was followed by a test array in which the squares reappeared, and on 50% of the trials one of the squares changed color. In this task, participants were instructed to indicate by button press response whether the test array was the same as or different from the memory array. For both the passive (WM−) and active (WM−) task variants (Figure 1a,b), the 2,000-ms delay was followed only by the prestimulus interval for the next trial. During the passive (WM−) task variant, participants were instructed to simply look at the squares as they appeared on the screen and were intermittently asked to rate neutral images on a pleasantness scale from 1–5 to ensure adequate task engagement. Finally, during the active (WM−) task variant, participants were instructed to attend to the images and press a button when they detected a target color appear among the squares in the visual array (which occurred on 10% of trials). Participants' responses were not speeded, and accuracy was at or near 100% for all participants (see Results). To avoid a memory requirement for this task, the target color was represented as a square that remained continuously present at the top center of the screen throughout this condition. The target color was randomly selected and remained constant throughout the condition for each participant. Target-present trials were excluded from further analysis to eliminate the impact of motor potentials during the measurement period. For all participants, the task variants were administered in the following order in the same testing session: passive (WM−), active (WM−), then active (WM+), each of which contained six blocks of 24 trials (144 trials total; 48 trials per set size). The order of the conditions was fixed to minimize the impact of previous task instruction from the previous condition on α/β-ERD measurement (see Discussion).

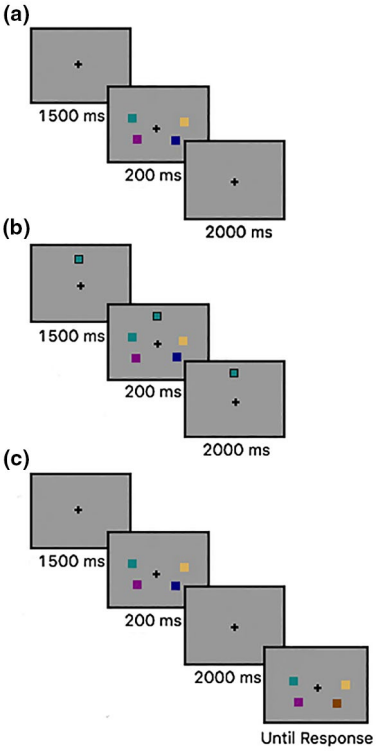

FIGURE 1 Trial sequence for each of three task variants: (a) passive (WM−); (b) active (WM−); (c) active (WM+). In the active (WM−) task variant, the target color was continuously presented at the top of the screen to eliminate a memory requirement

2.3 | EEG recording and analysis

The EEG was recorded continuously from 58 scalp electrodes at a sampling rate of 1,000 Hz with a Brain Products active electrode recording system (Brain Products GmbH). The EEG was low-pass filtered online at 200 Hz and referenced to a single electrode placed on the tip of the nose. Vertical and horizontal electro-oculogram were recorded with three electrodes: two lateral to the external canthi and one below the left eye. Finally, two electrodes were placed on the mastoids, to which the EEG was rereferenced offline.

Offline data processing was conducted in MATLAB (MathWorks, Inc., Natick, MA) using EEGLAB (Delorme & Makeig, 2004) and ERPLAB (Lopez-Calderon & Luck, 2014) toolboxes. Following rereferencing to the average of

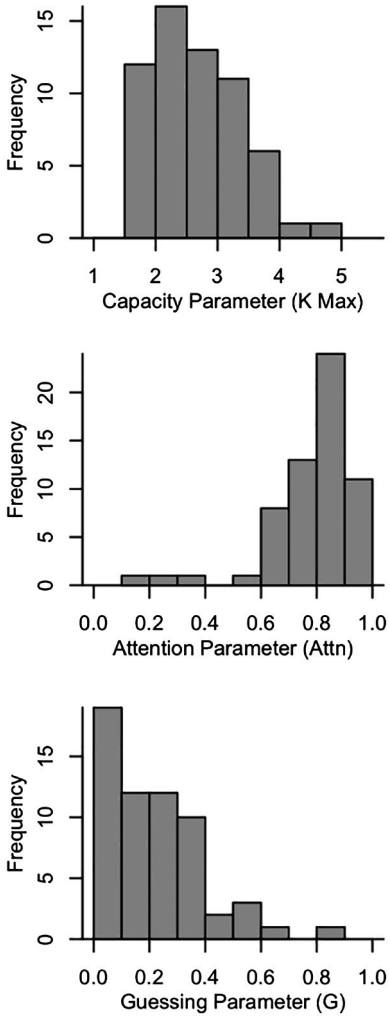

FIGURE 2 Distribution of behavioral parameters extracted from active (WM+) task variant: working memory capacity (K_{MAX}), probability that participant was paying attention on a given trial (Attn), and the probability that a participant was likely to make a "change" guess on uncertain trials (Guess)

the left and right mastoid electrodes, data were segmented into 4-s epochs (1,500 ms prestimulus to 2,500 poststimulus) and baseline corrected to the mean prestimulus voltage. Bad electrodes were identified using visual inspection and were interpolated. Independent component analysis (ICA) was then conducted to detect and remove components from the data that were associated with eye movements and blinks. Following ocular correction, artifact rejection was performed by using a series of algorithms built into ERPLAB. Any epochs with (a) amplitudes exceeding ±200 μV at any point in the epoch, or (b) peak-to-peak amplitudes that exceeded ±150 μV within a 200-ms moving window were marked for rejection. Finally, visual inspection of the data was conducted to eliminate remaining artifacts. The above artifact correction and rejection procedures resulted in an average of 75.62%, 71.15%, and 78.50% of trials retained for passive (WM−), active (WM−), and active (WM+) task variants, respectively. To measure the task-evoked power within the four frequency bands, time-frequency analysis was conducted on single trials by convolving a Hanning-tapered three-cycle Morlet wavelet with the EEG from each channel. Power was measured from the alpha (9–13 Hz) and beta (14–30 Hz) frequency bands and was baseline corrected to the proportional change in poststimulus power relative to the 1,500 ms before the onset of the sample array on a logarithmic scale (dB).

2.4 | Measurement window selection

We did not have a specific a priori hypothesis regarding the time window of the relevant effect for α/β-ERD. Therefore, to identify the temporal boundaries of the measurement period, the following steps were taken: first, power from all frequencies was averaged across set sizes, within two electrode clusters: a posterior cluster (O1, Oz, O2, PO7, PO3, POz, PO4, PO8, P7, P5, P3, P1, Pz, P2, P4, P6, P8) and a frontal cluster (Fp1, Fp2, AF7, AF3, AFz, AF4, AF8, F7, F5, F3, F1, Fz, F2, F4, F6, F8). Second, each participant's average power within these electrode clusters was transformed into a *t* score representing the number of standard deviations of change from baseline power. Finally, *t* scores from all 60 participants and for all three conditions were averaged. The temporal boundaries of the measurement window for the three conditions were identified by establishing the period of greatest deviance from the baseline distribution for alpha and beta, separately (see online supporting information, Figure S1). Using this method, α-ERD measurement windows were 174–999 ms poststimulus (posterior electrodes) and 174–809 ms poststimulus (frontal electrodes). The β-ERD measurement windows were identical for both frontal and posterior electrode clusters: 142–603 ms poststimulus. The same measurement window was used for all three task variants.

3 | RESULTS

3.1 | Task performance

To quantify WM task performance, three parameters were extracted from the full set of behavioral responses in the active (WM+) task variant for each participant: working memory storage capacity (K_{MAX}); the probability that the participant was paying attention on a given trial (Attn); and the participant's bias to make a "change" guess on uncertain trials (Guess). This parameter estimation process was originally developed by Rouder and colleagues (2008), and the details of model fit can be found in the supporting information, Appendix S1. Figure 2 depicts the distribution of K_{MAX}, Attn, and Guess parameters for all 60 participants. Average (*SD*) K_{MAX}, Attn, and Guess values were 2.67 (0.72), 0.79

(0.15), and 0.22 (0.17), respectively. Although not of central interest for the present study, we also examined performance in the active (WM−) task variant. As expected, average task performance was near ceiling (99.8% accuracy), indicating that participants were adequately attending to the visual arrays during this condition.

3.2 | Alpha desynchronization

α-ERD (dB) was measured from the frontal and posterior electrode clusters and statistically compared across the three task conditions using two 3 × 3 (Set Size × Condition) repeated measures analyses of variance (ANOVAs; see Figures 3 and 4). In the posterior cluster, we found a

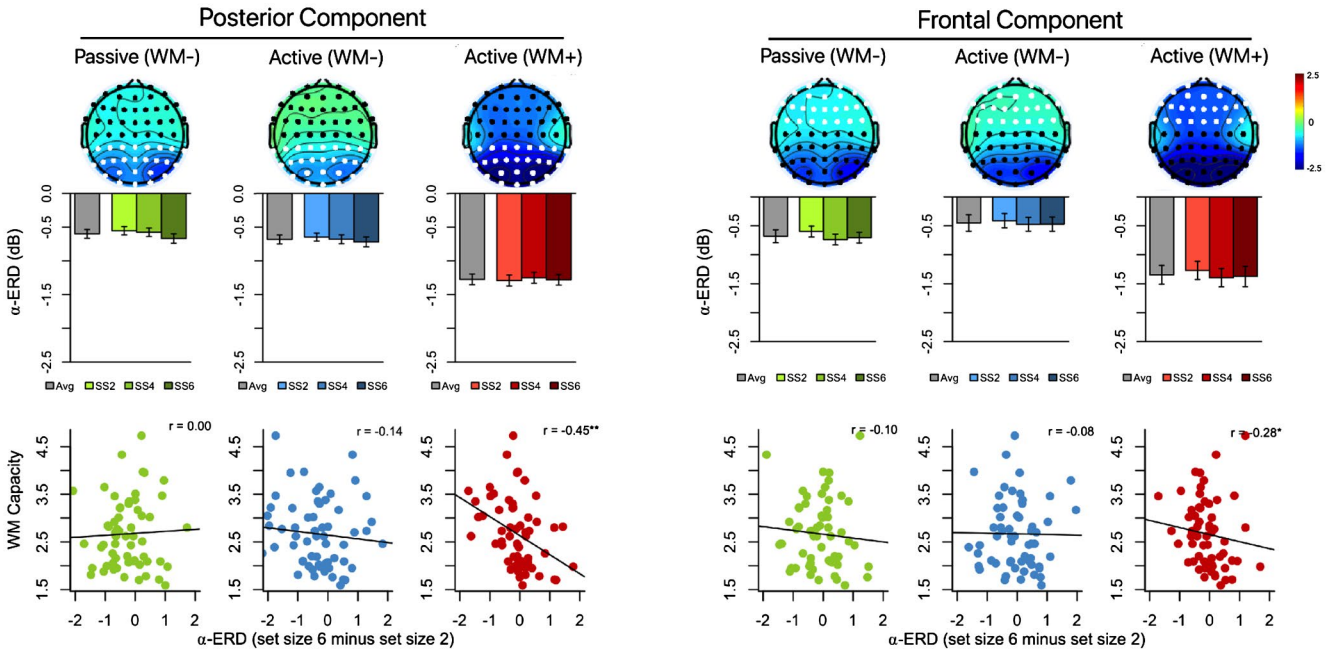

FIGURE 3 Alpha desynchronization (dB) for both the posterior and frontal component for each of the three task variants. Electrodes included in each component are depicted in white. Scalp maps represent average activity across measurement window. Correlations between alpha desynchronization and K_{MAX} for each of the three task variants are presented in the bottom panel

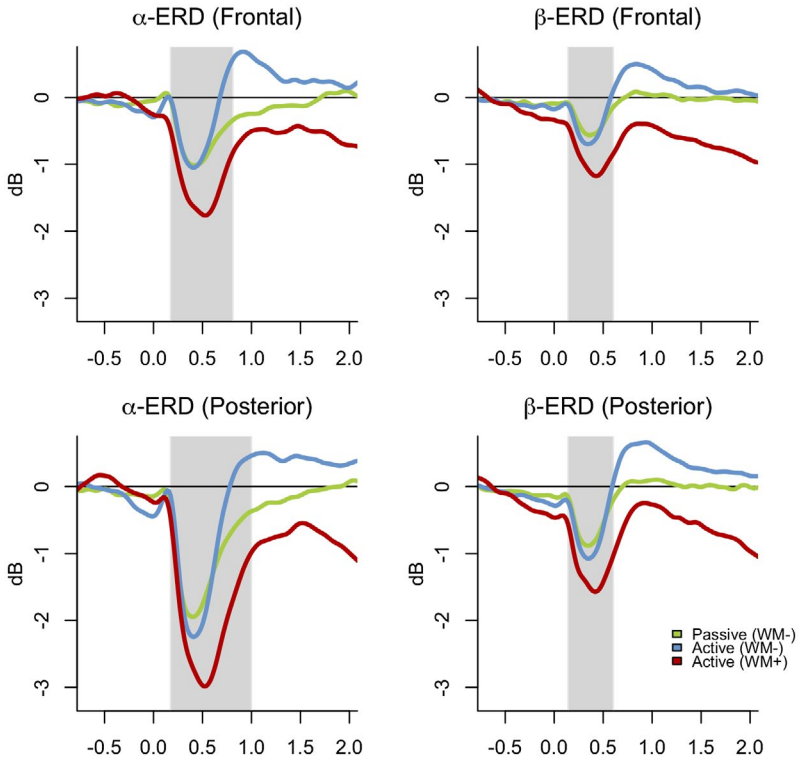

FIGURE 4 Time course of alpha and beta suppression for the passive (WM−) (green), active (WM−) (blue), and active (WM+) (red) task variants, separately for frontal and posterior electrode clusters. Gray panel represents the boundaries of the measurement period

significant main effect of set size ($F = 10.04$; $p < .001$), a significant main effect of task variant ($F = 37.56$; $p < .001$), and no interaction ($F = 1.09$; $p = .36$). Paired t tests revealed that alpha desynchronization was larger in the active (WM+) task variant compared to the passive (WM−) and active (WM−) task variants at all three set sizes (ts > 4.73; ps < .001). The passive (WM−) and active (WM−) task variants did not differ from one another at set sizes 4 or 6 (ts < 1.57; ps > .12), and α-ERD was significantly larger in the passive (WM−) task variant at set size 2 ($t = 2.40$; $p = .02$). In the frontal cluster, we again observed a main effect of task variant ($F = 27.20$; $p < .001$) but not set size ($F = 2.03$; $p = .14$) and no interaction ($F = 0.11$; $p = .98$). Paired t tests revealed that α-ERD was again larger in the active (WM+) task variant compared to the passive (WM−) and active (WM−) task variants at all three set sizes (ts > 4.20; ps < .001) and did not differ significantly between the passive (WM−) and active (WM−) task variants at any set size, although there was a trend-level effect of larger α-ERD in the passive (WM−) condition (ts < 1.97; ps > .05). Altogether, these results indicate that α-ERD is most robustly observed in the presence of a memory demand at both posterior and frontal electrode locations.

We next examined the relationship between working memory capacity (K_{MAX}) and α-ERD. Given the non-normal distribution of K_{MAX} (Shapiro-Wilk test statistic = 0.95; $p < .05$), Spearman correlation coefficients were used to measure the strength of the relationship between K_{MAX} and the set size effect of α-ERD, which is the difference in α-ERD between supracapacity and subcapacity array sizes (i.e., set size 6 − set size 2), as has been done elsewhere (Erickson et al., 2017; Fukuda et al., 2015). Overall, we found that α-ERD was only significantly associated with K_{MAX} in the active (WM+) condition. K_{MAX} was significantly correlated with the set size effect of α-ERD in both posterior ($r = -.45$; $p < .001$) and frontal electrode sites ($r = -.28$; $p < .05$). Importantly, K_{MAX} was not significantly associated with the set size effect of α-ERD in either the passive (WM−) or active (WM−) task variants at either the frontal or posterior electrode sites (rs = −.14 to .00; ps > .28). The correlation between K_{MAX} and α-ERD was significantly larger in the active (WM+) task variant compared to the correlations from the passive (WM−) and active (WM−) task variants in the posterior (Fisher's r-to-zs > 2.09; $p < .05$) but not frontal electrode cluster (Fisher's r-to-zs < 1.16; ps > .12).

3.3 | Beta desynchronization

β-ERD (dB) was measured from the frontal and posterior electrode clusters and statistically compared across the three task conditions using two 3 × 3 (Set Size × Condition) repeated measures ANOVAs (see Figures 4 and 5). In the posterior cluster, we observed a main effect of task variant ($F = 74.28$; $p < .001$), a trend-level effect of set size ($F = 2.80$; $p = .07$), and no interaction ($F = 1.01$; $p = .41$). Paired t tests revealed that β-ERD was significantly larger in the active (WM+) task variant compared to either the passive (WM−) or active (WM−) task variant at all set sizes (ts > 7.43; ps < .001), but no significant difference in β-ERD was observed between the passive (WM−) and active (WM−) task variants (ts < 1.73; ps > .09). A similar pattern was observed in the frontal electrode cluster, with a main effect of condition ($F = 60.12$; $p < .001$), a trend-level effect of set size ($F = 2.58$; $p = .08$), and no interaction ($F = 0.90$; $p = .46$). Once again, paired t tests revealed that β-ERD was significantly larger in the active (WM+) task variant compared to the passive (WM−) and active (WM−) task variants at all set sizes (ts > 6.41; ps < .001), and that β-ERD from the passive (WM−) and active (WM−) task variants were not significantly different from one another (ts < 1.32; ps > .19). K_{MAX} was not significantly associated with the set size effect of β-ERD in any of the three task variants (rs = −.14 to .09; ps > .29).

4 | DISCUSSION

In the present study, we used a three-variant change detection paradigm to test two competing hypotheses: (a) α/β-ERD elicited by a change detection visual WM task reflects a cognitive subprocess that is specific to memory formation, or (b) α/β-ERD reflects an earlier (i.e., perceptual or attentional) process that is necessary, but not sufficient, for WM storage. Our primary finding was that α/β-ERD was significantly larger in the active (WM+) task variant than in task variants without a memory demand, passive (WM−) and active (WM−). Additionally, only modulation of alpha in the active (WM+) task variant was significantly associated with WM capacity (K_{MAX}). This correlation was significantly stronger in the active (WM+) compared to task variants without a WM component in the posterior electrode cluster. These findings suggest that a significant portion of the α/β-ERD signal elicited during a WM task is specific to memory formation and/or storage processes. Furthermore, it is this memory-elicited desynchronization that accounts for the relationship between K_{MAX} and alpha modulation during visual WM tasks.

The above observations eliminate the explanation that a nonspecific visual process such as encoding accounts for either (a) the α/β-ERD response during visual change detection, or (b) the relationship between α/β-ERD and WM capacity. However, the experimental design does not permit further parsing of memory-specific subprocesses to determine which of these contributes to α/β-ERD. Thus, the degree to which α/β-ERD reflects consolidation, maintenance/rehearsal, retrieval, or some combination of these has yet to be determined. One possibility is that α/β-ERD directly or indirectly supports memory consolidation,

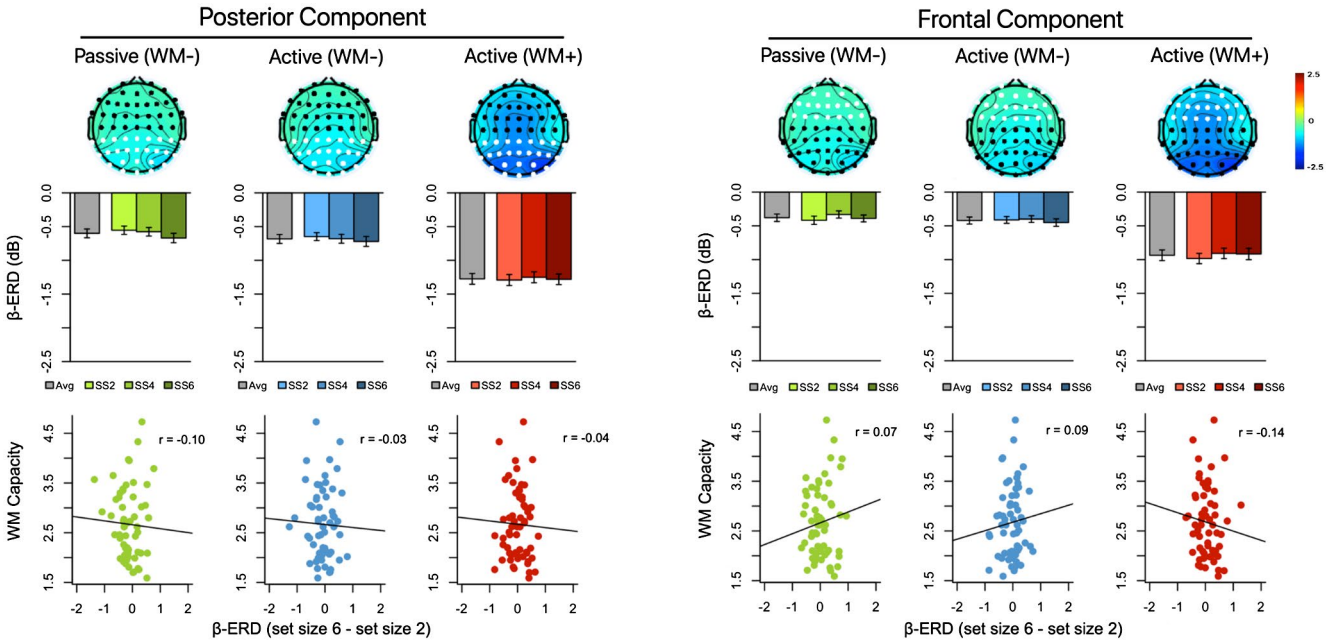

FIGURE 5 Beta desynchronization (dB) for each of the three task variants. Electrodes included in the component are depicted in white. Correlations between beta desynchronization and K_{MAX} are presented in the bottom panel

specifically; this interpretation is supported by the observation that between-task differences in α/β-ERD emerge early in the delay period during the large desynchronization peak immediately following the onset of the sample array (see Figure 4). However, the width of the α/β-ERD measurement window—approximately 460 to 825 ms in duration—is considerably longer than the 50-ms/item time course of consolidation estimated by Vogel, Woodman, and Luck (2006). Furthermore, Fukuda and Woodman (2017) have demonstrated that α-ERD tracks retrieval of items from long-term visual memory storage long after they have been consolidated. Additional studies are needed to directly test the role of α/β-ERD during the various phases of memory formation and recall.

Additional studies are also needed to clarify how α/β-ERD supports memory processes. Hanslmayr and colleagues (Hanslmayr, Staudigl, & Fellner, 2012) hypothesized that desynchronization supports memory formation by increasing the richness of the visual representations. According to this hypothesis, robust synchronization within a neural network carries highly redundant information within that signal; by contrast, desynchronization increases the entropy of the signal, thus increasing the amount of information that can be encoded by neuronal populations. This explanation seems unlikely to account for the present findings, however, as both the active (WM−) and active (WM+) task variants presumably required a similar degree of representational richness in order to discriminate between the sample array colors (active (WM−) task variant) and remember them (active (WM+) task variant).

Yet, another hypothesis proposes that items are gated into memory by gamma bursts during the oscillatory trough of the alpha rhythm. According to this view, when alpha is desynchronized, its magnitude is asymmetrically suppressed such that the oscillatory peaks become smaller and the troughs become larger; in this way, gamma bursts become longer and items in memory are more robustly maintained (Jensen, Gips, Bergmann, & Bonnefond, 2014). The pattern of results from the present study is consistent with this view of the role of α-ERD: it would be expected that longer gamma bursts (via larger asymmetrical suppression of alpha) would be observed in the active (WM+) task variant compared to the active (WM−) and passive (WM−) task variants, because longer gamma bursts would be necessary for robust consolidation and/or maintenance. Furthermore, it would be expected that only α-ERD in the active (WM+) task variant would be associated with WM capacity, since this is the only condition with sufficiently long periods of alpha-coupled gamma bursts. The present study was not designed to test this hypothesis directly, and so future studies are needed to evaluate the plausibility of this interpretation.

Finally, some limitations warrant mention. First, we did not control for differences in effort across the three task variants; therefore, it is possible that more desynchronization is reflective of more effortful engagement in the active (WM+) task variant compared to the passive (WM−) and active (WM−) task variants. It is noteworthy, however, that α/β-ERD was virtually identical between the passive (WM−) and active (WM−) task variants—this despite the fact that the active (WM−) task variant requires more cognitive

engagement than the passive (WM−) task variant. Therefore, there does not seem to be a consistent relationship between effort and α/β-ERD that could explain the observed pattern of results. Second, the response requirements were different across the three task variants. To mitigate the impact of motor responses on the delay period α/β-ERD, only trials for which no motor response occurred during the measurement period were included in the analysis; these included all passive (WM−) and active (WM+) trials, and all target- and response-absent active (WM−) trials. However, the impact task demands on any preparatory motor activity could not be controlled for using the present task design and should be taken into consideration when interpreting these results. Third, it should be noted that alpha modulation in particular likely serves a more complex function in the gating and manipulation of information stored in memory than is captured by the present analysis. Evidence from the literature regarding the impact of distractors and retro-cuing on alpha modulation suggests that it may also play a key role in protection of items in WM storage against distraction (Bonnefond & Jensen, 2012; Janssens, De Loof, Boehler, Pourtois, & Verguts, 2018) and WM updating (Manza, Hau, & Leung, 2014). Thus, the observations here that α/β-ERD plays a primary role in memory storage should be interpreted within a larger framework of how modulation of these frequency bands serves to process visual information.

ORCID

Molly A. Erickson https://orcid.org/0000-0002-5311-4402

REFERENCES

Astrand, E. (2018). A continuous time-resolved measure decoded from EEG oscillatory activity predicts working memory task performance. *Journal of Neural Engineering*, *15*(3), 036021–12. https://doi.org/10.1088/1741-2552/aaae73

Banerjee, S., Snyder, A. C., Molholm, S., & Foxe, J. J. (2011). Oscillatory alpha-band mechanisms and the deployment of spatial attention to anticipated auditory and visual target locations: Supramodal or sensory-specific control mechanisms? *Journal of Neuroscience*, *31*(27), 9923–9932. https://doi.org/10.1523/JNEUROSCI.4660-10.2011

Bashivan, P., Bidelman, G. M., & Yeasin, M. (2014). Spectrotemporal dynamics of the EEG during working memory encoding and maintenance predicts individual behavioral capacity. *European Journal of Neuroscience*, *40*(12), 3774–3784. https://doi.org/10.1111/ejn.12749

Bonnefond, M., & Jensen, O. (2012). Alpha oscillations serve to protect working memory maintenance against anticipated distracters. *Current Biology*, *22*(20), 1969–1974. https://doi.org/10.1016/j.cub.2012.08.029

Chen, Y. G., Chen, X., Kuang, C. W., & Huang, X. T. (2015). Neural oscillatory correlates of duration maintenance in working memory. *Neuroscience*, *290*(C), 389–397. https://doi.org/10.1016/j.neuroscience.2015.01.036

Cowan, N., Elliott, E. M., Saults, J. S., Morey, C. C., Mattox, S., Hismjatullina, A., & Conway, A. R. A. (2005). On the capacity of attention: Its estimation and its role in working memory and cognitive aptitudes. *Cognitive Psychology*, *51*(1), 42–100. https://doi.org/10.1016/j.cogpsych.2004.12.001

Delorme, A., & Makeig, S. (2004). EEGLAB: An open source toolbox for analysis of single-trial EEG dynamics including independent component analysis. *Journal of Neuroscience*, *134*(1), 9–21. https://doi.org/10.1016/j.jneumeth.2003.10.009

Engle, R. W., Tuholski, S. W., Laughlin, J. E., & Conway, A. R. A. (1999). Working memory, short-term memory, and general fluid intelligence: A latent-variable approach. *Journal of Experimental Psychology General*, *128*(3), 309–331. https://doi.org/10.1037/0096-3445.128.3.309

Erickson, M. A., Albrecht, M. A., Robinson, B., Luck, S. J., & Gold, J. M. (2017). Impaired suppression of delay-period alpha and beta is associated with impaired working memory in schizophrenia. *Biological Psychiatry: Cognitive Neuroscience and Neuroimaging*, *2*(3), 272–279. https://doi.org/10.1016/j.bpsc.2016.09.003

Foster, J. J., Sutterer, D. W., Serences, J. T., Vogel, E. K., & Awh, E. (2016). The topography of alpha-band activity tracks the content of spatial working memory. *Journal of Neurophysiology*, *115*(1), 168–177. https://doi.org/10.1152/jn.00860.2015

Fukuda, K., Mance, I., & Vogel, E. K. (2015). α Power modulation and event-related slow wave provide dissociable correlates of visual working memory. *Journal of Neuroscience*, *35*(41), 14009–14016. https://doi.org/10.1523/JNEUROSCI.5003-14.2015

Fukuda, K., Vogel, E., Mayr, U., & Awh, E. (2010). Quantity, not quality: The relationship between fluid intelligence and working memory capacity. *Psychonomic Bulletin & Review*, *17*(5), 673–679. https://doi.org/10.3758/17.5.673

Fukuda, K., & Woodman, G. F. (2017). Visual working memory buffers information retrieved from visual long-term memory. *Proceedings of the National Academy of Sciences*, *114*(20), 5306–5311. https://doi.org/10.1073/pnas.1617874114

Gomar, J. J., Valls, E., Radua, J., Mareca, C., Tristany, J., del Olmo, F., … The Cognitive Rehabilitation Study Group. (2015). A multisite, randomized controlled clinical trial of computerized cognitive remediation therapy for schizophrenia. *Schizophrenia Bulletin*, *41*(6), 1387–1396. https://doi.org/10.1093/schbul/sbv059

Handel, B. F., Haarmeier, T., & Jensen, O. (2011). Alpha oscillations correlate with the successful inhibition of unattended stimuli. *Journal of Cognitive Neuroscience*, *23*(9), 2494–2502. https://doi.org/10.1162/jocn.2010.21557

Hanslmayr, S., Staudigl, T., & Fellner, M.-C. (2012). Oscillatory power decreases and long-term memory: The information via desynchronization hypothesis. *Frontiers in Human Neuroscience*, *6*, 74–12. https://doi.org/10.3389/fnhum.2012.00074

Ichihara-Takeda, S., Yazawa, S., Murahara, T., Toyoshima, T., Shinozaki, J., Ishiguro, M., … Nagamine, T. (2015). Modulation of alpha activity in the parieto-occipital area by distractors during a visuospatial working memory task: A magnetoencephalographic study. *Journal of Cognitive Neuroscience*, *27*(3), 453–463. https://doi.org/10.1162/jocn_a_00718

Janssens, C., De Loof, E., Boehler, C. N., Pourtois, G., & Verguts, T. (2018). Occipital alpha power reveals fast attentional inhibition of incongruent distractors. *Psychophysiology*, *55*(3), e13011. https://doi.org/10.1111/psyp.13011

Jensen, O., Gips, B., Bergmann, T. O., & Bonnefond, M. (2014). Temporal coding organized by coupled alpha and gamma oscillations prioritize visual processing. *Trends in Neurosciences*, *37*(7), 357–369. https://doi.org/10.1016/j.tins.2014.04.001

Jensen, O., & Mazaheri, A. (2010). Shaping functional architecture by oscillatory alpha activity: Gating by inhibition. *Frontiers in Human Neuroscience*, *4*, 186–188. https://doi.org/10.3389/fnhum.2010.00186

Lenartowicz, A., Mazaheri, A., Jensen, O., & Loo, S. K. (2018). Aberrant modulation of brain oscillatory activity and attentional impairment in attention-deficit/hyperactivity disorder. *Biological Psychiatry: Cognitive Neuroscience and Neuroimaging*, *3*(1), 19–29. https://doi.org/10.1016/j.bpsc.2017.09.009

Lopez-Calderon, J., & Luck, S. J. (2014). ERPLAB: An open-source toolbox for the analysis of event-related potentials. *Frontiers in Human Neuroscience*, *8*(4), 213–214. https://doi.org/10.3389/fnhum.2014.00213

Luck, S. J., & Vogel, E. K. (1997). The capacity of visual working memory for features and conjunctions. *Nature*, *390*(6657), 279–281. https://doi.org/10.1038/36846

Manza, P., Hau, C. L. V., & Leung, H.-C. (2014). Alpha power gates relevant information during working memory updating. *Journal of Neuroscience*, *34*(17), 5998–6002. https://doi.org/10.1523/JNEUROSCI.4641-13.2014

Pavlov, Y. G., & Kotchoubey, B. (2017). EEG correlates of working memory performance in females. *BMC Neuroscience*, *18*(1), 1–14. https://doi.org/10.1186/s12868-017-0344-5

Poch, C., Valdivia, M., Capilla, A., Hinojosa, J. A., & Campo, P. (2018). Suppression of no-longer relevant information in working memory: An alpha-power related mechanism? *Biological Psychology*, *135*, 112–116. https://doi.org/10.1016/j.biopsycho.2018.03.009

Roijendijk, L., Farquhar, J., van Gerven, M., Jensen, O., & Gielen, S. (2013). Exploring the impact of target eccentricity and task difficulty on covert visual spatial attention and its implications for brain computer interfacing. *PLOS One*, *8*(12), e80489. https://doi.org/10.1371/journal.pone.0080489

Rouder, J. N., Morey, R. D., Cowan, N., Zwilling, C. E., Morey, C. C., & Pratte, M. S. (2008). An assessment of fixed-capacity models of visual working memory. *Proceedings of the National Academy of Sciences*, *105*(16), 5975–5979. https://doi.org/10.1073/pnas.0711295105

Sauseng, P., Klimesch, W., Heise, K. F., Gruber, W. R., Holz, E., Karim, A. A., … Hummel, F. C. (2009). Brain oscillatory substrates of visual short-term memory capacity. *Current Biology*, *19*(21), 1846–1852. https://doi.org/10.1016/j.cub.2009.08.062

van Dijk, H., van der Werf, J., Mazaheri, A., Medendorp, W. P., & Jensen, O. (2010). Modulations in oscillatory activity with amplitude asymmetry can produce cognitively relevant event-related responses. *Proceedings of the National Academy of Sciences*, *107*(2), 900–905. https://doi.org/10.1073/pnas.0908821107

Vogel, E. K., Woodman, G. F., & Luck, S. J. (2006). The time course of consolidation in visual working memory. *Journal of Experimental Psychology: Human Perception and Performance*, *32*(6), 1436–1451. https://doi.org/10.1037/0096-1523.32.6.1436

Wechsler, D. (2011). *WASI-II: Wechsler abbreviated scale of intelligence* (2nd ed.). San Antonio, TX: Psychological Corporation.

Zammit, N., Falzon, O., Camilleri, K., & Muscat, R. (2018). Working memory alpha-beta band oscillatory signatures in adolescents and young adults. *European Journal of Neuroscience*, *25*, 2527–2536. https://doi.org/10.1111/ejn.13897

Zumer, J. M., Scheeringa, R., Schoffelen, J.-M., Norris, D. G., & Jensen, O. (2014). Occipital alpha activity during stimulus processing gates the information flow to object-selective cortex. *PLOS Biology*, *12*(10), e1001965–13. https://doi.org/10.1371/journal.pbio.1001965

SUPPORTING INFORMATION

Additional supporting information may be found online in the Supporting Information section at the end of the article.

Appendix S1
Figure S1

How to cite this article: Erickson MA, Smith D, Albrecht MA, Silverstein S. Alpha-band desynchronization reflects memory-specific processes during visual change detection. *Psychophysiology*. 2019;00:e13442. https://doi.org/10.1111/psyp.13442